Chemical Engineering Journal 162 (2010) 194–200

Contents lists available at ScienceDirect

Chemical Engineering Journal

journal homepage: www.elsevier.com/locate/cej

# Adsorption isotherm models and properties of $SO_2$ and NO removal by palm shell activated carbon supported with cerium (Ce/PSAC)

S. Sumathi, S. Bhatia, K.T. Lee, A.R. Mohamed*

*School of Chemical Engineering, Engineering Campus, Universiti Sains Malaysia, 14300 Nibong Tebal, Pulau Pinang, Malaysia*

ARTICLE INFO

*Article history:*
Received 23 February 2010
Received in revised form 11 May 2010
Accepted 11 May 2010

*Keywords:*
Palm shell activated carbon
$SO_2$
NO
Adsorption isotherm

ABSTRACT

The adsorption of $SO_2$ and NO onto palm shell activated carbon supported with cerium oxide (Ce/PSAC) was studied in a fixed bed adsorber. This paper reports the adsorption equilibrium of $SO_2$ and NO in a simulated flue gas on Ce/PSAC. The experimental results show that within the experimental conditions at different inlet concentration of $SO_2$/NO, the adsorption capacities of Ce/PSAC can be well fitted by Langmuir compared to Freundlich adsorption isotherms. The binary mixtures of $SO_2$ and NO at different initial concentration can be well-correlated by the extended Jain and Snoeyink (JS) Langmuir model compared to extended Langmuir model. The physical properties of Ce/PSAC were calculated and it was consistent with the isotherm parameters obtained from the adsorption results. The adsorption was controlled by physisorption.



## 1. Introduction

Combustion processes and its emission *i.e.* flue gas has been a long time setback to nature as well as human kind. It has been reported that $SO_2$ and NO contained in flue gas are the primary agents responsible for the acid rain and ground-layer ozone formation. Due to these factors, interest in reducing these emissions simultaneously has been increasing lately to save the global health. Among the famous reducing methods are dry-type methods such as selective catalytic reduction, adsorption and flue gas desulphurization [1–5].

Activated carbon as an agent for adsorption has been used for many years in many field. Gas-phase adsorption by activated carbon is a separation process in which adsorbate molecules are transferred to the pore surface of solid activated carbon [6]. Activated carbon is predominantly amorphous material that has large surface area and pore volume. Activated carbons are made from variety of starting material [7]. For gaseous removal, activated carbon made from bituminous coal and coconut are the prominent ones [8]. Currently palm shell-based activated carbon is introduced for gas phase applications because it has similar property as coconut shell [9].

Few discussions were made in the literature about adsorption behavior of $SO_2$, $O_2$, $CO_2$, $N_2$, $CH_4$ and $H_2S$ on palm shell activated carbon (PSAC) [10–14]. However none have been reported on NO removal or simultaneous removal of $SO_2$ and NO. Moreover these researchers did not study the adsorption kinetics using model isotherms. Bae and Lee [15], examined the adsorption kinetics of 8 different gases ($O_2$, $H_2$, $N_2$, Ar, CO, $CO_2$, $SO_2$ and $CH_4$) on a carbon molecular sieve using three different isotherms, *i.e.* Dubunin–Radushkevich (DR), Langmuir and Freundlich–Langmuir (LF). Juray et al. [16] developed a transient kinetic model using Langmuir ideal surface and Elovich real surface model for simultaneous adsorption of NO and SO over Na/γ-AlO sorbent.

In this study, the most commonly used adsorption isotherm equations *i.e.* Langmuir and Freundlich were used to describe single gas adsorption of $SO_2$ and NO over Ce/PSAC. A modified extended Langmuir (MEL) was used to predict the binary mixture. Different inlet concentrations (*i.e.* 1000–2500 mg/l of $SO_2$ and 100–700 mg/l of NO) and equilibrium temperatures (*i.e.* 100–300 °C) were used to describe the adsorption isotherm and heat of adsorption.

## 2. Materials and methods

### 2.1. Preparation of sorbent

The PSAC was prepared by physical activation using $CO_2$ gas. The details of the preparation method are reported elsewhere [17]. Prior to the impregnation process, PSAC was sieved to a size of 1 mm. The PSAC was subjected to pore volume impregnation by cerium metal nitrate. First the PSAC was impregnated with cerium metal nitrate ($Ce(NO_3)_3{\cdot}6H_2O$) of an appropriate concentration to obtain around 10 wt% of metal content per gram of PSAC (10 ml of 10 wt% metal solution/g of PSAC). In this study cerium nitrate from Fluka was used as the metal precursors. During the impreg-

* Corresponding author. Tel.: +60 45996410; fax: +60 45941013.
*E-mail addresses:* chrahman@eng.usm.my, sumesethu@yahoo.com (A.R. Mohamed).

1385-8947/$ – see front matter © 2010 Elsevier B.V. All rights reserved.
doi:10.1016/j.cej.2010.05.028

nation, the solution of metal nitrate was continuously mixed with PSAC for 5 h. Then the samples were heated to 70 °C while being constantly stirred until the liquid was totally evaporated. After that the samples were dried in an oven at 110 °C for a period of 12 h. Finally, the prepared samples were heat-treated at 400 °C for 4 h in the presence of argon to form the reduced sorbents in oxide form. The selection of 10 wt% concentration of cerium was based on our preliminary study. Ce/PSAC denotes a sample impregnated with 10 wt% of cerium nitrate which has been calcined.

### 2.2. Activity test

The simultaneous removal activity of the prepared sorbent was carried out in a fixed bed adsorber. The schematic diagram of the experimental setup has been reported previously [18]. The prepared Ce/PSAC sorbent (1.0 g) was placed on borosilicate glass wool (0.05 g) in the center of the adsorber. A stream of gaseous mixture representing the simulated flue gas, containing $SO_2$ (2000 mg/l) (50%), NO (500 mg/l) (11%), $O_2$ (10%), and $N_2$ (29%) as the balance, was passed through the prepared sorbents. The feed flow through the adsorber was controlled at 150 ml/min. The GHSV of the system is 23,527 $h^{-1}$. The inlet and outlet concentrations of $SO_2$ and NO were measured using a wall-mounted flue gas analyzer (Electrochemical Gas Sensor Technology, IMR5000/400, Environmental Equipment Inc., USA) before and after adsorption activity. The concentrations of $SO_2$/NO were recorded from the first point of $SO_2$/NO detected in the effluent until it reaches the breakthrough point. It was continuously monitored for every minute. The column is taken to be at equilibrium when the effluent concentration levels off at or near the feed concentration. This situation indicates 100% of breakthrough. The gas flow through the adsorption column was continued for an additional time after the breakthrough time to ensure that adsorption equilibrium was reached. The activity of the sorbent towards $SO_2$/NO was expressed by $SO_2$/NO adsorption capacity, which is defined by the breakthrough curves ($C/C_o$ versus $t$). $C/C_o$ is a dimensionless factor, where $C$ is the outlet concentration of $SO_2$/NO (mg/l) from the adsorber, $C_o$ is the initial concentration of $SO_2$/NO (mg/l) and $t$ is the adsorption time (min). Each and every experimental run was repeated at least three times to increase the precision of the results, and only the average value was reported throughout this study. The repeatability was found to be sufficiently high with relative error less than 5%.

To study the effect of $SO_2$/NO adsorption capacity over Ce/PSAC, the feed concentration of $SO_2$ and NO was varied from 1000 to 2500 mg/l and 100 to 700 mg/l respectively. When $SO_2$ was varied, NO was fixed at 500 mg/l and when NO was varied $SO_2$ was fixed at 2000 mg/l. For the model fitting the adsorber temperature was set to 150 °C. This temperature was found to yield the best simultaneous removal of $SO_2$ and NO by Ce/PSAC from the previous study [19]. An adsorber temperature of 100–300 °C was used to study the heat of adsorption.

## 3. Results and discussion

### 3.1. Characteristics of Ce/PSAC

From the previous studies [17], it was found that PSAC without modification/impregnation with metal oxides could only remove $SO_2$ successfully. Hence in order to achieve simultaneous removal of $SO_2$ and NO, it was deduced that PSAC should be impregnated with metal oxides. PSAC impregnated with cerium oxide was found to yield the best simultaneous removal of $SO_2$ and NO compared to other metal oxides [20]. The characteristics and proximate analysis of PSAC and Ce/PSAC are shown in Table 1.

**Table 1**
The characteristics and proximate analysis of PSAC and Ce/PSAC.

| Characteristics | PSAC | Ce/PSAC |
|---|---|---|
| BET surface area ($m^2$/g) | 1250 | 807 |
| Micropore volume ($cm^3$/g) | 0.399 | 0.330 |
| Average pore diameter (Å) | 16.0 | 15.0 |
| Solid density (g/$cm^3$) | 1.693 | 1.961 |
| Proximate analysis (wt%) | | |
| Carbon | 85.2 | 63.9 |
| Moisture | 7.4 | 18.1 |
| Volatile | 4.3 | 8.6 |
| Ash | 3.1 | 9.4 |

### 3.2. Single-component $SO_2$ and NO adsorption equilibrium

The simplest and still useful isotherm is the Langmuir equation [21], which is based on constant adsorption energy independent of surface coverage. When the adsorption equilibrium data do not fit well on linear coordinates, the Freundlich isotherm is probably the equation most commonly used. The Freundlich model [21], which is usually applied in a strictly empirical sense, can be of theoretical interest in terms of adsorption onto an energetically heterogeneous surface assuming a heterogeneous valence distribution. Hence in this study the pure component *i.e.* $SO_2$/NO was analyzed based on Langmuir and Freundlich isotherm.

Langmuir isotherm is expressed as

$$q = q_s \frac{K_L C}{1 + K_L C} \tag{1}$$

where $C$ is the initial concentration of the adsorbate (mg/l), $q$ is the adsorption capacity of adsorbent (mg/g), $q_s$ (mg/g) is Langmuir constant related to adsorption capacity and $K_L$ is Langmuir constant related to rate of adsorption (l/mg). Hence a linearized plot of $C/q$ vs. $C$ gives a straight line with slope of $(1/q_s)$ and intercept of $(1/q_s K_L)$.

Freundlich isotherm is expressed as

$$q = K_F C^{1/n} \tag{3}$$

where $q$ (mg/g) is the adsorption capacity of adsorbent, $C$ (mg/l) is the initial adsorbate concentration, $K_F$ is adsorption or distribution coefficient for Freundlich isotherm (mg/g(l/mg)$^{1/n}$) and $n$ is the Freundlich constant and $1/n$ is the heterogeneity factor. The isotherm is usually used for special case of heterogeneous surface energy in which it is characterized by the heterogeneity factor $1/n$. A plot of ln($q$) vs. ln($C$) enables the constant $K_F$ and exponent $1/n$ to be determined. The magnitude of the exponent $n$ gives an indication of the favorability of adsorption. Whereby, values $n > 1$ represent favorable adsorption condition.

The adsorption capacity of Ce/PSAC for $SO_2$ and NO was determined by a dynamic mass balance, which requires numerical integration of the data. Using the breakthrough curve data from an adsorption breakthrough run, the time equivalent to the total or stoichiometric capacity of the column for a particular adsorbate is calculated numerically integrating the following equation:

$$t_t = \int_0^\infty \left(1 - \frac{C}{C_o}\right) dt$$

where $t_t$ is the time equivalent to the total or stoichiometric capacity, $t$ is the time, $C$ is the concentration of adsorbate at time $t$, and $C_o$ is the feed concentration of adsorbate. With $t_t$ determined, the amount of adsorbate adsorbed by adsorbent (the adsorption capacity) is calculated at non-STP condition from the following equation [22]:

$$q = \frac{Q_f t_t y_f}{m_c}$$

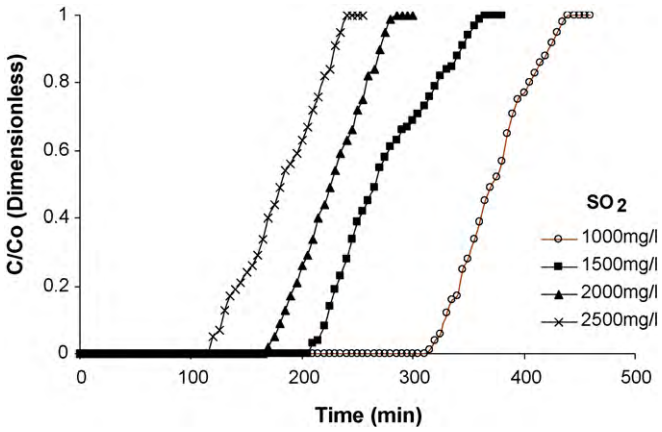


**Fig. 1.** $SO_2$ removal at different initial concentration.

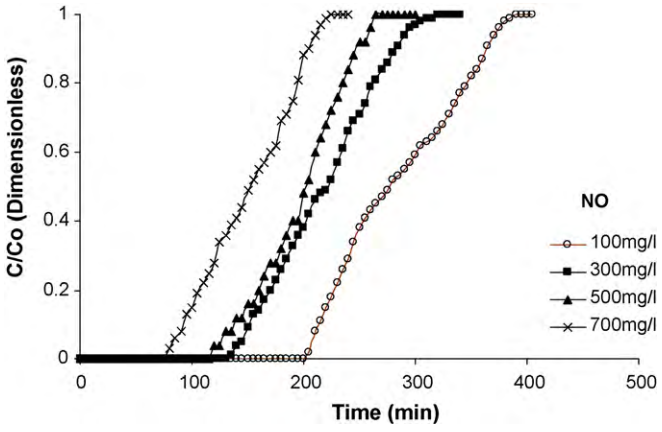


**Fig. 2.** NO removal at different initial concentration.

where $q$ is the adsorbent adsorption capacity, $y_f$ is the mole fraction of adsorbate in the feed, $Q_f$ is the volumetric feed flow rate at STP, and $m_c$ is the mass of adsorbent used inside the bed.

Figs. 1 and 2 show the breakthrough curves of $SO_2$ and NO at different initial concentrations. Table 2 shows the sorption capacity of $SO_2$ and NO at different initial concentration. From Figs. 1 and 2 and Table 2 it was noticed that, for low concentrations of $SO_2$ or NO, a relatively small amount of $SO_2$ (89.33 mg/g) and NO (0.93 mg/g) were adsorbed and a longer time was required to reach breakthrough point. Tsai et al. reported a similar trend of breakthrough curve for VOC removal at different initial concentration [23]. However, for a $SO_2$ concentration of 2500 mg/l, the amount adsorbed was high as 120.25 mg/g and the breakthrough time was shorter. The same phenomenon was observed for NO concentration at 700 mg/l. These data suggested that the sorption capacity and sorption rate of PSAC–Ce are dependent on the concentration of the adsorbate. A similar finding was reported by Lua and Guo [24] for $SO_2$ adsorption by PSAC.

Thus these data are substituted into the isotherms *i.e.* Langmuir and Freundlich. Fig. 3(a) and (b) shows the linearized plot of $(C/q)$ vs. $C$ for different initial concentration for $SO_2$ and NO respectively for Langmuir isotherm. Fig. 4(a) and (b) shows the plot of $\log q$ vs. $\log C$ for different initial concentration for $SO_2$ and NO respectively for Freundlich isotherm. Table 3 shows the calculated numerical parameters of Langmuir and Freundlich from Figs. 3 and 4. A comparative study based on the parameters of the respective isotherms in Table 3 was done.

It was observed that Langmuir isotherm fits well for $SO_2$ or NO adsorption by Ce/PSAC compared to Freundlich isotherm under the

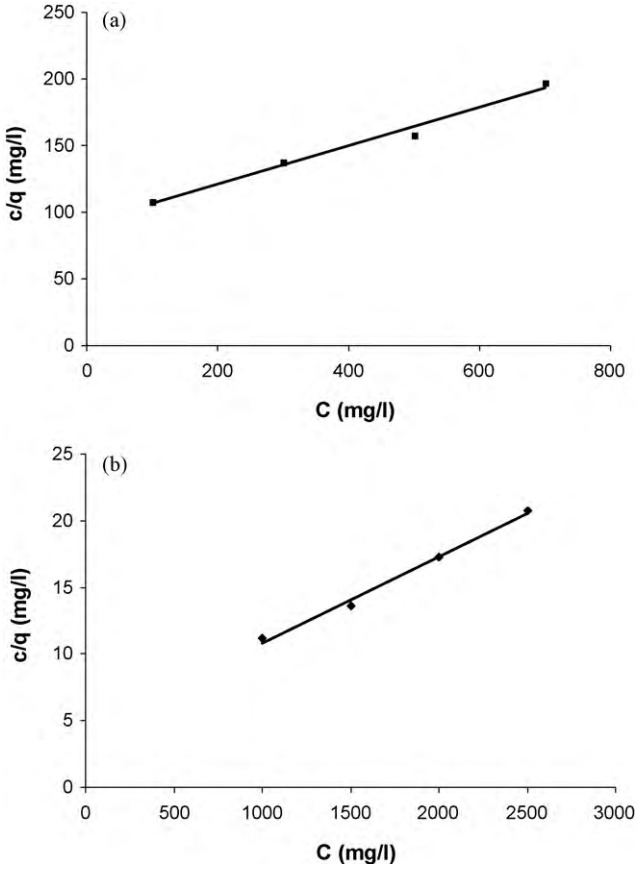


**Fig. 3.** Langmuir plot of (a) $SO_2$ adsorption on PSAC–Ce, (b) NO adsorption on PSAC–Ce.

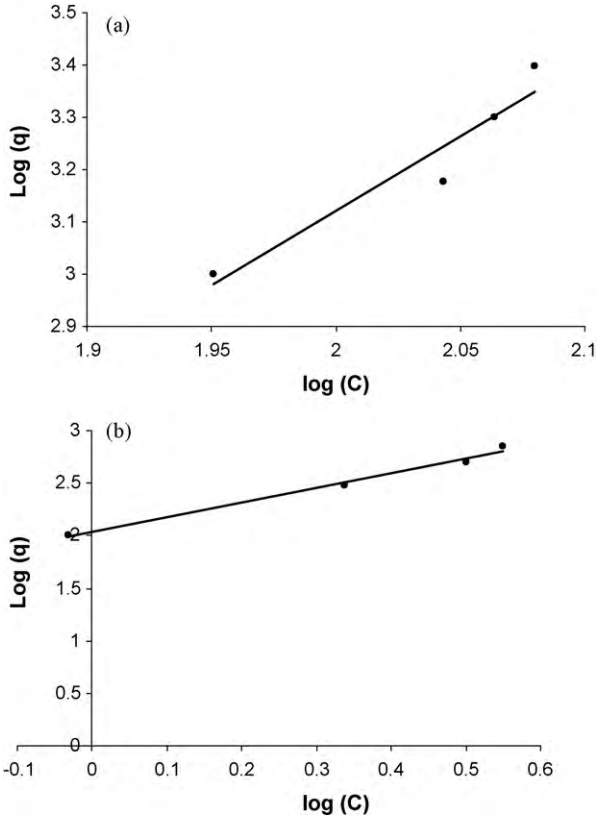


**Fig. 4.** Freundlich plot of (a) $SO_2$ adsorption on PSAC–Ce, (b) NO adsorption on PSAC–Ce.

**Table 2**
Sorption capacity of $SO_2$ and NO by PSAC–Ce at different initial concentration.

| Initial concentration (mg/l) $SO_2$/NO | Breakthrough time (min) | | Sorption capacity (mg pollutant/g PSAC–Ce) | |
|---|---|---|---|---|
| | $SO_2$ | NO | $SO_2$ | NO |
| 1000/100 | 455 | 405 | 89.33 | 0.93 |
| 1500/300 | 375 | 315 | 110.43 | 2.18 |
| 2000/500 | 295 | 275 | 115.83 | 3.17 |
| 2500/700 | 245 | 220 | 120.25 | 3.55 |

**Table 3**
Calculated numerical parameters and constants of Langmuir and Freundlich for $SO_2$ and NO adsorption.

| Gas adsorbed | Langmuir | | | Freundlich | | |
|---|---|---|---|---|---|---|
| | $K_L$ (l/mg) | $q_s$ (mg/g) | $R^2$ | $K_F$ (mg/g (l/mg)$^{1/n}$) | $n$ | $R^2$ |
| $SO_2$ | 0.001496 | 153.85 | 0.992 | 0.0229 | 0.4208 | 0.9175 |
| NO | 0.001567 | 6.92 | 0.987 | 107.5474 | 0.7168 | 0.9903 |

concentration range studied by comparing the correlation coefficient ($R^2$) value. The $R^2$ value of Langmuir isotherm plot was very close to the most favorable value of $R^2 = 1$ whereas for Freundlich isotherms it was found that it could not fit well with the $SO_2$ sorption by Ce/PSAC. NO sorption data at different initial concentration of NO vs. sorption capacity could fit the Freundlich isotherm well with $R^2 > 0.99$. However the calculate $n$ value for both gaseous were lower than 1. This means that the adsorption was unfavorable which is impossible in this case. Thus Freundlich isotherm could not represent the adsorption isotherm of $SO_2$ and NO from Ce/PSAC.

In order to justify that the Langmuir model fits well with the single-component data, the linear transform model is illustrated in Fig. 5(a) and (b). The predicted data matched well with the experimental data for $SO_2$ as well as NO with a correlation coefficient factor of $R^2 > 0.95$. This suggests that the Langmuir isotherm can provide a reasonable description and analysis of the data for the single gas sorption.

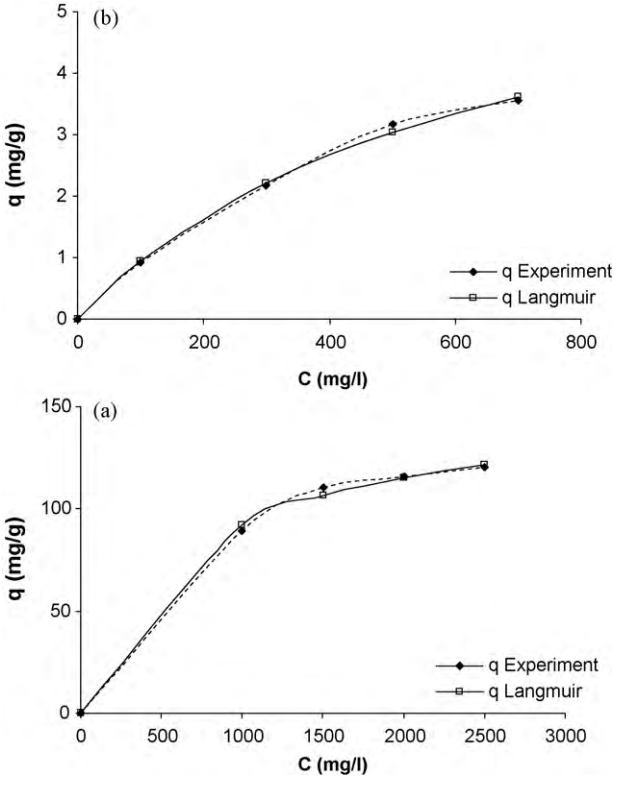


**Fig. 5.** Continued single-component Langmuir isotherms vs. experimental data derived by linearization for (a) $SO_2$ and (b) NO.

### 3.3. Multi-component $SO_2$ and NO adsorption equilibrium

An extended Langmuir equation has been developed for competitive multi-component adsorption by Butler and Ockrent in 1930 [25]. This model assumes a homogeneous surface with respect to the energy of adsorption, no interaction between adsorbed species, and that all sites are equally available to all adsorbed species. Extended Langmuir isotherm is expressed as

$$q_i = \frac{K_L q_o C_i}{1 + \sum_{j=1}^{N} K_{Lj} C_j} \quad (5)$$

where is $q_{,i}$ is the equilibrium of the component $i$, $N$ is the number of the components, $C_j$ ($j = 1,2,3\ldots,n$) is the equilibrium concentration of each component, while $K_{L,i}$ and $q_{o,i}$ are Langmuir constants obtained from the corresponding single adsorbate adsorption isotherm.

The extended Langmuir competitive model (Eq. (5)), which assumes that competition between different components is only depended on the adsorbate concentrations ratio, can be applied in order to predict the adsorption behavior of a material in a multi-component system, using the single-component parameters. In many cases, the adsorption constants of the individual isotherms fail to describe the interactions between adsorbate ions in a binary system. The addition of further correction parameters to the classical competitive Langmuir equation (Eq. (5)) makes the model capable to depict the complexity of the adsorption process. The modified extended Langmuir equation is given as [26]

$$q_i = \frac{q_{o,i} K_{L,i} (C_i / n_{ii})}{1 + \sum_{j=1}^{N} K_{Lj} (C_j / n_{ij})} \quad (6)$$

where $K_{L,i}$, $q_{o,i}$ are derived from the corresponding single-component Langmuir equations and $n_{ij}$ is the correction parameter of species $i$ and $j$, which is characteristic of each species and depends on the concentrations of all the other components in the system.

The single-component parameter sets for the two gases, obtained using the Langmuir model methods, were substituted into Eq. (6) to enable prediction of the binary component isotherms using the extended Langmuir isotherm. Examples of the model predictions compared with experimentally measured results are presented in Table 4. It was noticed that the well-known extended Langmuir model developed from the basic Langmuir model did not fit this set of experimental data to predict multi-component adsorption. The data shows the extended Langmuir model could predict the NO adsorption accurately

**Table 4**
$q$ (experiment), $q$ (predicted) and $R^2$ values for the extended Langmuir isotherm using Langmuir isotherm parameter sets.

| Concentration (mg/l) | $q$ (mg/g) (experiment) | $q$ (mg/g) (predicted) | Correlation coefficient ($R^2$) |
|---|---|---|---|
| $SO_2$ | | | |
| 1000 | 89.33 | 196.46 | 0.3125 |
| 1500 | 110.43 | 231.32 | Not fit |
| 2000 | 115.83 | 253.85 | |
| 2500 | 120.25 | 269.60 | |
| NO | | | |
| 100 | 0.938 | 0.926 | 0.999 |
| 300 | 2.213 | 2.180 | |
| 500 | 3.041 | 2.990 | |
| 700 | 3.620 | 3.557 | |

with $R^2 = 0.9672$, but then not for $SO_2$ adsorption by Ce/PSAC ($R^2 = 3.125$).

The extended Langmuir isotherm is based on the same assumptions as the single-component Langmuir isotherm. Whereby there should be no interaction between the gases and an equal competition for the adsorption sites occur during the adsorption. From previous research data report earlier [27], it was found that $SO_2$ gas creates a competition with NO to be adsorbed on to the active sites of Ce/PSAC. Thus this is clearly proven in this case and it must be assumed that there is a significant interaction and competition occurring, resulting in the extended Langmuir model failing to apply to this system. The results in Table 4 also indicate that $q$ (predicted) for $SO_2$ gas does not match the $q$ (experiment) because $SO_2$ gas is the one that creates the competition towards NO gas.

Thus in this study case, the adsorption constants of the individual isotherms fail to describe the interactions between the gases with the extended Langmuir model for the multi-component adsorption. The addition of correction factor to the classical competitive Langmuir equation (Eq. (6)) can make the model capable to depict the complexity of the adsorption process. The extended Langmuir model should take into consideration the presences of other gases in the flow that can affect the apparent affinity of a particular gas for the adsorption on an active site. In many cases, due to the occurrence of other gases in the flow, the maximum uptake does not remain constant. Thus in this study an improved and modified version of extended Langmuir model with the factor $Q_o$, added to the existing extended Langmuir model was done. This model was proposed by Jain and Snoeyink in 1973 [28] and is named as JS modified Langmuir, which for a binary system can be written as

$$q_{O1} = \frac{(q_{o,1} - q_{o,2})K_{L,1}C_1}{1 + K_{L,1}C_1} + \frac{q_{o,2}K_{L,1}C_1}{1 + K_{L,1}C_1 + K_{L,2}C_2} \quad (7)$$

$$q_{O1} = \frac{q_{o,2}K_{L,2}C_2}{1 + K_{L,1}C_1 + K_{L,2}C_2} \quad (8)$$

The first term in Eq. (7) can be related to the fraction of species (1) that is sorbed without competition, while the second term in Eq. (8) corresponds to the fraction of ions (1) that adsorb in competition with ions of species (2). It must be noted that all parameters in Eqs. (7) and (8) can be determined from single-component isotherms.

Table 5 shows the multi-component isotherm $q$ (experiment), $q$ (predicted) and $R^2$ values for the MEL isotherm using single Langmuir isotherm parameter sets. From Table 5 it can be clearly seen that the MEL model developed from the basic extended Langmuir model predicted the multi-component adsorption competently.

It was observed that the $q$ (predicted) was almost similar to one reported by the experiment. This data verifies that MEL model fits well with the set of experimental data in this study. MEL model could predict the $SO_2$ and NO adsorption accurately with $R^2 > 0.95$. The error difference between the experiment and predicted data was less than 7% and 5% for $SO_2$ and NO respectively. Fig. 6(a) and (b) shows the MEL model fit in graphical form. The predicted data matched well with the experimental data for $SO_2$ as well as NO with a correlation coefficient factor of $R^2 > 0.95$. This suggests that the MEL isotherm models exhibit excellent reproduction of the experimental data at the whole concentration range for the multi-component adsorption of $SO_2$ and NO from flue gas. The first term in the MEL equation can be related to the fraction of species (1) *i.e.* $SO_2$ that is sorbed without competition, while the second term corresponds to the fraction of ions (1) that adsorb in competition with ions of species (2) *i.e.* NO.

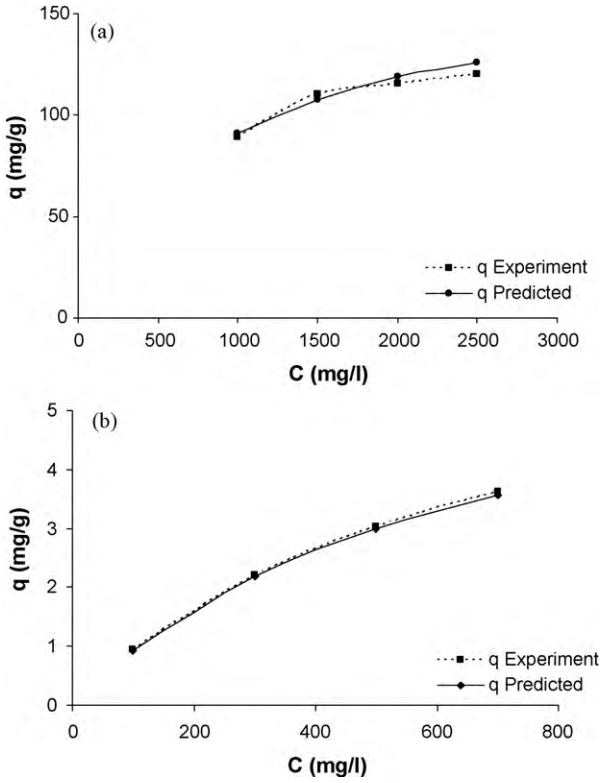


**Fig. 6.** Multi-component MEL model vs. experimental for (a) $SO_2$ and (b) NO sorption equilibrium.

Thus this model can predict the competitive adsorption of $SO_2$ and NO from the simulated flue gas with acceptable fitting results. According to the JS modified Langmuir adsorption model [28], the presence of other gases in the flow, affects, not only the shape of the isotherm curve, due to changes in apparent gas affinity for the active sites, but also the maximum uptake, $Q_o$ of each component. This is why the model can predict binary adsorption isotherms with relative success using single-solute parameters, even if the difference in the adsorbate capacities is quite large.

**Table 5**
$q$ (experiment), $q$ (predicted) and $R^2$ values for the modified extended Langmuir (MEL) isotherm using Langmuir isotherm parameter sets.

| Concentration (mg/l) | $q$ (mg/g) (experiment) | $q$ (mg/g) (predicted) | Error (%) | Correlation coefficient ($R^2$) |
|---|---|---|---|---|
| $SO_2$ | | | | |
| 1000 | 89.33 | 90.80 | 1.6 | 0.9666 |
| 1500 | 110.43 | 107.60 | 2.5 | |
| 2000 | 115.83 | 119.32 | 3.0 | |
| 2500 | 120.25 | 128.36 | 6.7 | |
| NO | | | | |
| 100 | 0.938 | 0.926 | 1.2 | 0.999 |
| 300 | 2.213 | 2.180 | 3.3 | |
| 500 | 3.041 | 2.990 | 1.7 | |
| 700 | 3.620 | 3.557 | 1.7 | |

**Table 6**
Parameters of Langmuir isotherm and vant Hoff equation for adsorption of $SO_2$ and NO on PSAC–Ce at various temperatures.

| Adsorbate | Equilibrium temperature | Langmuir parameters | | $R^2$ | Vant Hoff parameters | |
|---|---|---|---|---|---|---|
| | (°C) | $q_s$ (mg/g) | $K_L$ (l/mg) | | $\Delta H$ (kJ/mol) | $\Delta S$ (kJ/mol K) |
| $SO_2$ | 100 | 153.85 | 0.001496 | 0.99 | 8.28 | 0.032 |
| | 150 | 153.88 | 0.002052 | 0.98 | | |
| | 200 | 98.04 | 0.001771 | 0.98 | | |
| | 250 | 97.08 | 0.001011 | 0.99 | −18.68 | −0.093 |
| | 300 | 82.65 | 0.000779 | 0.97 | | |
| NO | 100 | 6.92 | 0.001567 | 0.99 | | |
| | 150 | 7.87 | 0.001696 | 0.97 | | |
| | 200 | 7.97 | 0.001762 | 0.98 | 2.49 | 0.047 |
| | 250 | 9.67 | 0.002011 | 0.99 | | |
| | 300 | 4.53 | 0.002584 | 0.98 | | |

### 3.4. Heat of adsorption

The heat of adsorption was assumed to be independent of temperature and was evaluated by the vant Hoff equation [21] as

$$\ln K_L = \ln \frac{q_e}{C_e} = \frac{\Delta S^\circ}{R} - \frac{\Delta H^\circ}{RT} \quad (9)$$

whereby $\Delta H$ is the heat of adsorption (enthalpy change) (J/mg), $\Delta S$ is entropy change, $T$ is the solution temperature (K), $K_L$ is Langmuir constant and $R$ is gas constant, 8.314 J/mol K. Thus, the entropy $\Delta S^\circ$ (kJ/mol K), and enthalpy $\Delta H^\circ$ (kJ/mol) values of an adsorption process can be calculated from the slope and the intercept of $\ln K_L$ vs. $1/T$ plot. The linearity between $\ln K_L$ and $1/T$ is also an indication that the adsorption is an endothermic process [29].

Earlier it was found that Langmuir isotherm could be used to predict the adsorption isotherm of $SO_2$ and NO by Ce/PSAC. Thus to predict the heat properties of $SO_2$ and NO adsorption, Langmuir constants, $q_s$ and $K_L$, based on the experimental data estimated from the breakthrough data of different temperature effect on $SO_2$ and NO adsorption from the previous study were used [19]. The Langmuir constants were then substituted in the vant Hoff equation. The Langmuir constants, $q_s$ and $K_L$ of $SO_2$ and NO at different temperatures are shown in Table 6. To calculate $\Delta H$ and $\Delta S$ a plot of $\ln K_L$ versus $1/T$ was done. The results are given in Table 6.

The Langmuir constants, $q_s$ and $K_L$, were determined from the breakthrough data of different temperature effect on $SO_2$ and NO adsorption and are presented in Table 6. As shown in Table 6, the experimental data could be reasonably fitted by the Langmuir equation with correlation coefficients ($R^2$) in the range of 0.96–0.98. Table 6 indicates that the maximum adsorption capacity, $q_s$ and $K_L$, for Ce/PSAC decreases at 300 °C for both NO and $SO_2$. This tendency is reasonable because it is known that at higher temperature the adsorption affinity will be reduced. It was noticed that for NO at temperatures below 300 °C the process was endothermic. This is because increase in temperature can increase the rate of reaction of NO with Ce reduction in Ce/PSAC. Whereas for $SO_2$, temperatures of 100 and 150 °C shows an endothermic adsorption and temperatures from 200 to 300 °C was exothermic. This is because at these temperatures $SO_2$ could not be adsorbed by Ce/PSAC physically or chemically. For an exothermic reaction at constant pressure, the change in enthalpy is equal to the energy released in the reaction, including the energy retained in the adsorption and lost through expansion against its surroundings.

In a similar manner, for an endothermic reaction, the system's change in enthalpy is equal to the energy absorbed in the reaction, including the energy lost by the adsorption and gained from compression from its surroundings. Thus a relatively easy way to determine whether or not a reaction is exothermic or endothermic is by looking at the sign of $\Delta H$.

Therefore in this case for $SO_2$ gas adsorption by Ce/PSAC at initial temperature the $\Delta H$ was positive, the reaction was endothermic, that is heat is absorbed by the adsorption process due to the products of the reaction having a greater enthalpy than the reactants. This could be one of the main reasons for poor removal of NO at lower temperatures. On the other hand at higher temperatures the $\Delta H$ was negative, the reaction is exothermic, that is the overall decrease in enthalpy is achieved by the generation of heat. The exothermic adsorption processes may be due the weakening of sorptive forces between the active sites on the Ce/PSAC and $SO_2$. Thus as temperature increased, the physical bonding between the organic compounds and the actives of the adsorbent are weakened. This can be clearly seen for $SO_2$ at temperatures more than 150 °C and NO at 300 °C.

For NO at temperatures below 300 °C the $\Delta H$ was positive, the reaction was endothermic. This data proves that NO molecules need more energy in order to be adsorbed by Ce/PSAC and why the adsorption of NO was more favorable at higher temperatures with Ce/PSAC. NO was reduced by Ce/PSAC at higher temperature. Increase in temperature could also increase the rate of diffusion of NO molecules across the external boundary layer and the internal pores of Ce/PSAC. So this could be also the reason why the enthalpy was low even at higher temperature for NO.

The range of the change of enthalpy for chemisorption is $-50\,\text{kJ/mol} > \Delta H > -800\,\text{kJ/mol}$ [30] whereas for physisorption is

below −50 kJ/mol. Referring to Table 6, all the $\Delta H$ values obtained were found to be less than −50 kJ/mol, which directly lead to a conclusion of an adsorption process controlled by physisorption.

From Table 6 it appears that the value of $\Delta S$ for $SO_2$ was greater to NO. $\Delta S$ describes the randomness at the solid–gas interface during the adsorption. Which proves that at lower temperatures $SO_2$ could be adsorbed better compared to NO by Ce/PSAC. The negative value of $\Delta S$ for $SO_2$ at higher temperatures corresponds to a decrease in the degree of freedom of the $SO_2$ adsorbed. As observed earlier higher temperature provokes the adsorption of NO thus this state indirectly decreases the freedom of $SO_2$ to be adsorbed onto Ce/PSAC.

## 4. Conclusions

The adsorption characteristics of $SO_2$ and NO on Ce/PSAC were investigated. From the experimental results and data regression analysis, the adsorption of $SO_2$ and NO can be well fitted by the Langmuir isotherm for single gas ($SO_2$/NO) compared to Freundlich. For binary mixture ($SO_2$ and NO) the extended JS Langmuir model correlated well compared to extended Langmuir model. Temperature plays an important role in the adsorption of $SO_2$ and NO by Ce/PSAC. Higher temperature (>250 °C) deters the adsorption properties of Ce/PSAC. Lower temperatures (<150 °C) are favored for $SO_2$ adsorption. It was concluded that the overall adsorption process of $SO_2$ and NO by Ce/PSAC was controlled by physisorption.

## Acknowledgements

The authors would like to acknowledge Ministry of Science, Technology and Innovation (MOSTI) Malaysia, Universiti Sains Malaysia (814004) RU Grant and Yayasan Felda (6050095) Long Term Grant for funding and supporting this project.

## References

[1] G. Xie, Z. Liu, Z. Zhu, Q. Liu, J. Ge, Z. Huang, Simultaneous removal of $SO_2$ and $NO_x$ from flue gas using $CuO/Al_2O_3$ catalyst sorbent I. Deactivation of SCR activity by $SO_2$ at low temperatures, J. Catal. 224 (2004) 36–41.
[2] S.M. Jeong, S.D. Kim, Removal of $NO_x$ and $SO_2$ by $CuO/Al_2O_3$ sorbent/catalyst in a fluidized bed reactor, Ind. Eng. Chem. Res. 39 (2000) 1911–1916.
[3] S.V. Pisupati, S. Bhalla, Influence of calcium content of biomass-based materials on simultaneous $NO_x$ and $SO_2$ reduction, Environ. Sci. Technol. 42 (7) (2008) 2509–2514.
[4] W. Nimmo, A.A. Patsias, E.G. Hampartsoumian, P.T. Williams, Simultaneous reduction of $NO_x$ and $SO_x$ emissions from coal combustion by calcium magnesium acetate, Fuel 83 (2004) 149–155.
[5] Y. Wang, Z. Liu, L. Zhan, Z. Huang, Q. Liu, J. Ma, Performance of an activated carbon honeycomb supported $V_2O_5$ catalyst in simultaneous $SO_2$ and NO removal, Chem. Eng. Sci. 59 (2004) 5283–5290.
[6] R.C. Bansal, J.B. Donnet, F. Stoeckli, Active Carbon, Marcel Dekker Inc., New York, 1988.
[7] O. Ioannidou, A. Zabaniotou, Agricultural residues as precursors for activated carbon production—a review, Renew. Sust. Energy Rev. 11 (9) (2007) 1966–2005.
[8] K.E. Noll, V. Gournis, W.S. Hou, Adsorption Technology for Air and Water Pollution Control, Lewis, Chelsea, MI, USA, 1991.
[9] W.M.A.W. Daud, W.S.W. Ali, Comparison on pore development of activated carbon produced from palm shell and coconut shell, Bioresour. Technol. 93 (2004) 63–69.
[10] M.K. Aroua, W.M.A.W. Daud, C.Y. Yin, D. Adinata, Adsorption capacities of carbon dioxide, oxygen, nitrogen and methane on carbon molecular basket derived from polyethyleneimine impregnation on microporous palm shell activated carbon, Sep. Purif. Technol. 62 (3) (2008) 609–613.
[11] J. Guo, Y. Luo, A.C. Lua, R. Chi, Y. Chen, X. Bao, S. Xiang, Adsorption of hydrogen sulphide ($H_2S$) by activated carbons derived from oil-palm shell, Carbon 45 (2007) 330–336.
[12] J. Guo, A.C. Lua, Microporous activated carbons prepared from palm shell by thermal activation and their application to sulphur dioxide adsorption, J. Colloid Interface Sci. 251 (2002) 242–247.
[13] J. Guo, A.C. Lua, Adsorption of sulphur dioxide onto activated carbon prepared from oil-palm shells with and without pre-impregnation, Sep. Purif. Technol. 30 (2003) 265–273.
[14] C.L. Aik, G. Jia, Preparation and characterization of activated carbons from oil-palm stones for gas-phase adsorption, Colloids Surf. 179 (2001) 151–162.
[15] Y.S. Bae, C.H. Lee, Sorption kinetics of eight gases on a carbon molecular sieve at elevated pressure, Carbon 43 (2005) 95–107.
[16] D.W. Juray, K.D. Asit, H.H. Geraldine, B.M. Guy, Development of a transient kinetic model for the simultaneous adsorption of $SO_2$–NO over $Na\gamma/Al_2O_3$ sorbent, Ind. Eng. Chem. Res. 40 (1) (2001) 119–130.
[17] S. Sumathi, S. Bhatia, K.T. Lee, A.R. Mohamed, Optimization of microporous palm shell activated carbon production for flue gas desulphurization: experimental and statistical studies, Bioresour. Technol. 100 (2009) 1614–1621.
[18] S. Sumathi, S. Bhatia, K.T. Lee, A.R. Mohamed, Performance of an activated carbon made from waste palm shell in simultaneous adsorption of SOx and NOx of flue gas at low temperature, Sci. China Ser. E: Tech. Sci. 52 (2009) 1–6.
[19] S. Sumathi, S. Bhatia, K.T. Lee, A.R. Mohamed, Cerium impregnated palm shell activated carbon (Ce/PSAC) sorbent for simultaneous removal of $SO_2$ and NO—process study, Chem. Eng. J. 162 (2010) 51–57.
[20] S. Sumathi, S. Bhatia, K.T. Lee, A.R. Mohamed, Selection of best impregnated palm shell activated carbon (PSAC) for simultaneous removal of $SO_2$ and $NO_x$, J. Hazard. Mater. 176 (2010) 1093–1096.
[21] I.M. Richard, Principles of Adsorption and Reaction on Solid Surfaces, Wiley Inter-Science, Canada, 1996.
[22] C.N. Satterfield, Heterogeneous Catalysis in Practice, McGraw Hill Inc., New York, 1980.
[23] W.T. Tsai, C.Y. Chang, C.Y. Ho, L.Y. Chen, Adsorption properties and breakthrough model of 1,1-dichloro-1-fluoroethane on activated carbons, J. Hazard. Mater. B69 (1999) 53–66.
[24] A.C. Lua, J. Guo, Adsorption of sulfur dioxide on activated carbon from oil-palm waste, J. Environ. Eng. 127 (2001) 895–901.
[25] S.J. Allen, G. Mckay, J.F. Porter, Adsorption isotherm models for basic dye adsorption by peat in single and binary component systems, J. Colloid Interface Sci. 280 (2004) 322–333.
[26] M. Alimohamadi, G. Abolhamd, A. Keshtkar, Pb(II) and Cu(II) biosorption on *Rhizopus arrhizus* modeling mono- and multi-component systems, Miner. Eng. 18 (2005) 1325–1330.
[27] S. Sumathi, S. Bhatia, K.T. Lee, A.R. Mohamed, $SO_2$ and NO simultaneous removal from simulated flue gas over cerium-supported palm shell activated at lower temperatures-role of cerium on NO removal, Energy Fuel 24 (2010) 427–431.
[28] S.K. Papageorgiou, F.K. Katsaros, E.P. Kouvelos, N.K. Kanellopoulos, Prediction of binary adsorption isotherms of $Cu^{2+}$, $Cd^{2+}$ and $Pb^{2+}$ on calcium alginate beads from single adsorption data, J. Hazard. Mater. 162 (2009) 1347–1354.
[29] A.L. Myers, Thermodynamics of adsorption in porous materials, AIChE 48 (1) (2002) 145–160.
[30] D.D. Do, Adsorption Analysis: Equilibria and Kinetics. Vol. 2, Series on Chemical Engineering, Imperial College Press, Australia, 1998.